Effects of Hypoxia in Intestinal Tumors on Immune Cell Behavior in the Tumor Microenvironment

Luping Zhang
Department of Gastroenterology. The First Hospital of Jilin University.Chang chun.China.
Shaokun Wang
Department of Emergency. The First Hospital of Jilin University.Chang chun.China.
Yachen Wang
Department of Gastroenterology. The First Hospital of Jilin University.Chang chun.China
Weidan Zhao
Department of Gastroenterology. The First Hospital of Jilin University.Chang chun.China
Yingli Zhang
Department of Gastroenterology. The First Hospital of Jilin University.Chang chun.China.
Nan Zhang (zhangnan@jlu.edu.cn)
Jilin University First Hospital https://orcid.org/0000-0003-2152-6274
Hong Xu
Department of Gastroenterology. The First Hospital of Jilin University.Chang chun.China

Research

Keywords: Colorectal cancer, Hypoxia, Immune cell infiltration, Tumor microenvironment

Posted Date: December 22nd, 2020

DOI: https://doi.org/10.21203/rs.3.rs-131685/v1

Abstract

Background: Imbalanced nutritional supply and demand in the tumor microenvironment often leads to hypoxia. The subtle interaction between hypoxia and immune cell behavior plays an important role in tumor occurrence and development. However, the functional relationship between hypoxia and the tumor microenvironment remains unclear. Therefore, we aimed to investigate the effect of hypoxia on the intestinal tumor microenvironment**.**

Method: We extracted the names of hypoxia-related genes from the Gene Set Enrichment Analysis (GSEA) database and screened them for those associated with the prognosis of colorectal cancer, with the final list including *ALDOB*, *GPC1*, *ALDOC*, and *SLC2A3*. Using the sum of the expression levels of these four genes, provided by The Cancer Genome Atlas (TCGA) and Gene Expression Omnibus (GEO) databases, and the expression coefficients, we developed a hypoxia risk score model. Using the median risk score value, we divided the patients in the two databases into high- and low-risk groups.GSEA was used to compare the enrichment differences between the two groups.We used the CIBERSORT computational method to analyze immune cell infiltration.Finally,the correlation between these five genes and hypoxia was analyzed.

Result: The prognosis of the two groups differed significantly, with a higher survival rate in the low-risk group than in the high-risk group.We found that the different risk groups were enriched by immune-related and inflammatory pathways. We identified activated CD4 memory T cells and M0 macrophages in TCGA and GEO databases and found that *CCL2/4/5*, *CSF1*, and *CX3CL1* contributed toward the increased infiltration rate of these immune cell types. Finally, we observed a positive correlation between the five candidate genes' expression and the risk of hypoxia, with significant differences in the level of expression of each of these genes between patient risk groups.

Conclusion: Overall, our data suggest that hypoxia is associated with the prognosis and rate of immune system infiltration in patients with colorectal cancer. This finding may improve immunotherapy for colorectal cancer.

Background

Since Stephen Paget proposed the "seed and soil" theory of cancer development and tumor metastasis[1], the understanding of the tumor microenvironment has gradually deepened. Several components of the tumor microenvironment contribute toward tumor occurrence and development[2,3]. An imbalance between nutrient supply and demand within the tumor often leads to hypoxia, glucose deficiency, and consequently an acidic tumor microenvironment[4]. Specifically, tumor cells can use immune escape mechanisms to drive metastasis and invasion in anoxic environments[5]. This has increased research interest into the relationship between hypoxia and the tumor immune microenvironment.

Hypoxia can reduce the activity of various immune cells in the tumor microenvironment and the production of corresponding immune stimulators to increase the release of suppressors and the expression of immune checkpoint inhibitors[5,6], suggesting a close relationship between hypoxia and immune cells.

This study aimed to investigate the relationship between hypoxia-related genes and the immune microenvironment of colorectal cancer by (1) quantifying the influence of these genes on the tumor immune microenvironment, (2) screening hypoxia-related genes associated with intestinal tumor prognosis, (3) developing a hypoxia risk score model, (4) validating the model's ability to predict patient prognosis and risk using data from The Cancer Genome Atlas (TCGA) and Gene Expression Omnibus (GEO) databases, (5) identifying the enrichment of model-related pathways, (6) using the hypoxia risk score as the entry point to explore differences in the infiltration rate of immune cells, and (7) identifying genes that affect immune cell infiltration to evaluate the relationship between hypoxia risk score and the tumor immune microenvironment.

Materials And Methods

Raw data

The intestinal cancer-related RNA-sequencing and clinical data used in this study were obtained from TCGA (https://portal.gdc.cancer.gov/) and GEO (gse39582) databases.

Construction and grouping of the hypoxia model

The screening of hypoxia-related genes identified the genes independently related to the prognosis of intestinal cancer. We then multiplied the expression levels of each gene in TCGA and GEO databases by their respective expression coefficients, with the resulting sum defined as the risk score for each patient. Based on the median risk score value, the patients in the two databases were divided into high- and low-risk groups for the follow-up evaluations.

Survival analysis

The survival and survminer R packages (The R Foundation for Statistical Computing, Vienna, Austria) were used to analyze the prognosis of 445 and 579 patients in TCGA and GEO databases, respectively. Patients in TCGA database were followed up for 12 years, while those in the GEO database were followed up for 16 years. The Kaplan–Meier method was used to plot the survival curves, and the log-rank test was used to evaluate the statistical significance between them, with p-values of < 0.05 considered statistically significant.

Receiver operating characteristic curve analysis

The ROC curve analysis was conducted using the survival, survminer, and timeROC packages in R. The 1-, 3-, and 5-year survival rates of patients in TCGA and GEO databases were evaluated. The areas under the ROC curve of the 1-, 3-, and 5-year survival rates increased gradually and exceeded 0.5, which was defined

as the threshold for the accurate prediction of survival by the model. The survival in both groups is shown as risk columns and risk curves in Fig. 2A–B.

Heat maps

In this study, heat maps of gene expression were drawn using the pheatmap package in R.

Protein-protein interaction network analysis

A network of anoxic genes was constructed using the STRING database. R software was used to select the 50 genes with the largest numbers of adjacent nodes for subsequent analysis.

Cox regression analysis

We applied the “survival” package in R and performed univariate Cox regression analysis to identify hypoxia-related genes that were closely related to prognosis. Univariate and multivariate prognostic analyses included factors such as age, sex, TNM stage, and the proposed risk score.

Correlations between gene expression and hypoxia risk

After screening for genes that play a key role in immune cell regulation, the ggplot2, GGPUBR, and ggExtra packages in R were used to analyze the correlations between gene expression and the risk of hypoxia, and the differences in expression levels between patients at high- and low-risk of hypoxia.

Gene Set Enrichment Analysis

We downloaded the HALLMARK gene set and gene symbols from the GSEA (https://www.gsea-msigdb.org/gsea/index.jsp) website to extract hypoxia-related genes. The entire transcriptome of all tumor samples was used for GSEA, and only gene sets with nominal p-values of < 0.05 and FDR q values of < 0.06 were considered significant.

Results

Extraction and screening of hypoxia-related genes

We first downloaded the hallmark gene sets. The gene symbol set was obtained from the Gene Set Enrichment Analysis (GSEA) website (https://www.gsea-msigdb.org/gsea/index.jsp), which provides the names of all hypoxia-related genes. We then used Search Tool for the Retrieval of Interacting Genes/Proteins (STRING) (http://string-db.org/cgi/input.pl), a protein-protein interaction (PPI) network database, to construct a model of PPIs between hypoxia-related genes (Fig. 1A). By counting the number of adjacent nodes of each protein, we identified the core genes. The top 50 core genes with adjacent nodes are presented in Fig. 1B. We then downloaded the intestinal tumor gene expression data and associated clinical information available from TCGA database. We extracted the data on hypoxia-related gene expression and screened genes associated with prognosis using univariate Cox regression analysis (Fig. 1C). Among the identified genes, *ALDOB* was associated with a low risk, while five genes (*GPC1,*

ALDOC, ENO2, SERPINE1, and *SLC2A3*) were associated with a high risk of developing tumor malignancy. The multivariate Cox regression analysis of genes associated with patient prognosis revealed four genes (Fig. 1D) that were then used to construct prognostic models. These four genes (*ALDOB*, *GPC1, ALDOC*, and *SLC2A3*) had model coefficients of -0.1574, 0.2994, 0.2647, and 0.2074, respectively.

Effects of hypoxia-related genes on prognosis

Multivariate Cox regression analysis identified four hypoxia-related genes associated with intestinal tumor prognosis, which were used for modeling. We multiplied the expression levels of these genes (as reported in TCGA and GEO databases) by the corresponding coefficients to obtain the risk score for each patient. The median risk score value was then used to divide the patients in TCGA database into high- and low-risk groups. The subsequent survival analysis revealed significant differences between the high- and low-risk groups ($p < 0.05$; Fig. 2A–B). Receiver operating characteristic (ROC) curve analysis was used to verify the accuracy of the survival estimates derived from the present model, showing a gradually increasing accuracy of predicting the 1-, 3-, and 5-year survival rates of patients included in TCGA database (Fig. 2C). The area under the ROC curve for the GEO database was greater than 0.05 (Fig. 2D), which indicated that the model accurately predicted the survival rate. To more intuitively evaluate the survival rate of patients in the high- and low-risk groups, we used risk histograms to show the differences in survival status between the two databases (Fig. 3A–B). We observed a higher proportion of surviving patients in the low-risk group than in the high-risk group. These results further demonstrated that our model effectively distinguished between high- and low-risk patients. We also analyzed the interactions between the hypoxia-related genes that were identified as affecting patient prognosis in the model (Fig. 3C–D). We further demonstrated the relationship between patient risk and survival using risk curves, in which the risk scores for both groups of patients were plotted (Fig. 3E–F). We observed a longer survival time in the low-risk group than in the high-risk group. Moreover, the number of deaths in the low-risk group decreased over time (Fig. 3G–H). Finally, we compared the expression level of each gene included in the model between the high- and low-risk groups using thermography (Fig. 3I–J).

Effects of different clinical characteristics on intestinal tumor prognosis

Clinical characteristics differ in the impact they have on patient prognosis. Thus, we analyzed the impact of clinical characteristics on the prognosis of patients included in TCGA and GEO databases. We first used univariate Cox regression analysis to evaluate the impact of clinical characteristics on the survival time and prognosis of patients included in the two databases (Fig. 4A–B). We found that patient sex affected neither survival nor prognosis, while other factors affected survival and prognosis and were associated with increased risk. However, the p-values of the risk score in our model were < 0.05 for patients in TCGA database, indicating that the risk score also affected patient prognosis and survival. In contrast, the p-values were > 0.05 for patients in the GEO database. Multivariate analysis of these factors showed that the p-values for age and tumor–node–metastasis (TNM) stage were all < 0.05, indicating that these variables were independent prognostic factors. We also observed differences in the expression levels of hypoxia-related genes between patients with different T stages included in the two databases

(Fig. 4E–H). The expression level of *SLC2A3* in different T stages (T1, T2, T3, and T4) differed significantly between patients in TCGA and GEO databases ($p < 0.05$).

Enrichment of pathways in hypoxia-related risk groups

We observed differences in the enrichment level of hypoxia-related genes and associated pathways between the high- and low-risk groups. To understand the level of pathway enrichment, we used GSEA software (UC San Diego, San Diego, CA, USA; Broad Institute, Cambridge, MA, USA) to compare the pathways between different risk groups. The high-risk group in TCGA database showed a large number of enriched pathways related to apoptotic and immune functions (Fig. 5A) compared with the low-risk group. Among these were apoptosis, hypoxia, interleukin (IL) 2/signal transducer and activator of transcription 5 (STAT5) signaling, IL6-STAT3 signaling, and the inflammatory response pathways. The other related pathways are shown in **Table 1** (**Stab. 1**). In contrast, the pathways enriched in the low-risk group mainly included those associated with oxidative phosphorylation and lipid metabolism, among others. The pathways with false discovery rate (FDR) values > 0.05 are shown in **Table 2**. The low-risk group of patients in the GEO database also showed the enrichment of apoptosis and IL2-STAT5 signaling pathways, in addition to, the p53 and peroxisome and phosphatidylinositol 3-kinase-mammalian target of rapamycin serine/threonine protein kinase B signaling pathways (Fig. 5B). The enrichment of other pathways is shown in **Table 3**. The high-risk group also showed the enrichment of the Hedgehog and Wnt/beta-catenin signaling pathways. Pathways with FDR values > 0.05 are shown in **Stab. 4**.

Immune cell infiltration

The results of the pathway enrichment analysis of hypoxia-related genes for both risk groups in TCGA and GEO databases showed the enrichment of pathways related to inflammation, immunity, and other factors. Based on these findings, we assessed the rate of immune cell infiltration in each risk group according to the constructed hypoxia-related gene model. Figure 5C–D shows the infiltration rate of immune cells in the high- and low-risk groups in TCGA and GEO databases, respectively. TCGA database showed differences in the infiltration rate of two types of immune cells in the high- and low-risk groups (Fig. 5E; $p < 0.05$). In contrast, the rate of infiltration of 10 types of immune cells differed between the high- and low-risk groups in the GEO database (Fig. 5F; $p < 0.05$). Among them, the infiltration rate of activated CD4 memory T cells and M0 macrophages differed between the high- and low-risk groups in both databases. Using the Tracking Tumor Immunophenotype online platform (http://biocc.hrbmu.edu.cn/TIP/index.jsp), we screened the immune-related genes for those that played important roles in the regulation of these two cell types. Heat maps were then drawn to visualize the expression of these genes relative to that of hypoxia-related genes in the high- and low-risk groups of patients in TCGA and GEO databases (Fig. 6A–B). The expression levels of *CCL2/4/5, CSF1*, and *CX3CL1* were significantly different between the high- and low-risk groups in both databases ($p < 0.05$). Next, we plotted the correlation curves between the expression levels of these five genes and the risk scores, which showed that the expression levels of these five genes were positively correlated with the patients' risk score. We also observed differences in the expression levels of these five genes between the high- and low-risk groups (Fig. 6C–L).

Discussion

Hypoxia is a feature of tumor physiology, specifically that of mechanisms associated with the acquisition of some malignant attributes, such as metastasis, invasion[7–9], and drug resistance[10]. In these processes, hypoxia-related genes act on the corresponding pathways or on the regulating immune cells. Hypoxia-inducible factor (HIF) is activated during hypoxia; some immunosuppressive factors, such as vascular endothelial growth factor, are HIF target genes, which affect both angiogenesis and immunosuppression[11]. Hypoxia also results in upregulated *EGFR* expression, which promotes ligand-independent epidermal growth factor receptor signaling[12,13]. This process increases the rate of tumor glycolysis, resulting in metabolic competition[14]. In our study, we screened for hypoxia-related genes in the gut and found that the core genes (*ALDOB*, *GPC1*, *ALDOC*, and *SLC2A3*) were closely related to patient prognosis. The rate of aldolase-B and fructose-bisphosphate B-driven fructose metabolism is significantly increased in patients with colon cancer and liver metastasis, and in those with colorectal villous polyps[15,16]. *GPC1* has also been shown to be overexpressed in various malignancies[17,18]. A recent study has reported *GPC1* enrichment in tumor-derived exosomes[17]. In melanoma, *NME1* has been shown to inhibit metastasis by activating *ALDOC* transcription[19]. Solute carrier family 2, member 3 can increase glucose uptake in anoxic cells and, thus, increase the rate of glycolysis. These findings suggest that hypoxia-related gene expression levels are closely related to tumor development and metabolism[20]; therefore, they were included in our hypoxia-related gene model.

With a deepening understanding of the mechanisms of hypoxia, its influence on tumor prognosis is also increasingly being understood[21,22]. To further investigate the relationship between the expression of hypoxia-related genes and patient prognosis, we evaluated patient prognosis by taking the product sum of the expression levels and the coefficients of *ALDOB*, *GPC1*, *ALDOC*, and *SLC2A3* in TCGA and GEO databases as the risk score. The prognosis of patients in the high- and low-risk groups differed significantly; the survival rate of patients in the low-risk group was significantly higher than that of their counterparts. However, the ROC curve analysis, which aimed to evaluate the accuracy of the survival estimates, showed that the curves obtained from the GEO database corresponded poorly to the observed prognosis. Thus, we also analyzed the influence of other factors, including age, sex, TNM staging, and our proposed risk score, on patient prognosis. We concluded that our proposed risk score showed a good correspondence to patient prognosis. However, the results of the multivariate analysis in the GEO database were not statistically significant. This finding suggests that the risk score alone cannot be used as an independent prognostic factor. The samples in the GEO database were all colorectal adenocarcinoma samples that had been obtained in France. Because the tumor type and region are very specific, these samples may not accurately reflect the relationship between hypoxia and colon cancer prognosis. Moreover, the prognosis of colon cancer is related to disease stage and clinical, histological, genetic, and molecular factors, among others. These factors should be considered in future studies.

We next applied GSEA to identify pathways enriched in the high- and low-risk groups in the two databases. We found that most of the enriched pathways were related to inflammation, immune

response, and apoptosis. Hypoxia and cell death in tumor tissue produce large amounts of cell debris and trigger the release of inflammatory factors, which can attract macrophages and monocytes, and can induce macrophage polarization. After polarization, macrophages secrete inflammatory factors[23]. These findings suggest a close relationship between hypoxia, inflammation, and the immune response. In addition, some apoptosis-related genes, such as p53, which is a tumor suppressor gene, are closely related to tumor apoptosis. Nilay *et al.*[24] found that mutations in p53 in gastric and esophageal cancer cells can induce hypoxia signaling. This finding was confirmed in a study involving nude mice[24].

The results of a large number of previous studies and those of the present study have shown that hypoxia can recruit immune cells in the tumor microenvironment. Hypoxia-induced tumor-derived cytokines, such as IL-10 and transforming growth factor-beta, can induce tumor-associated macrophages to differentiate into M2 macrophages with immunosuppressive effects[25]. When monocytes are stimulated by inflammatory factors, such as interferon-gamma and lipopolysaccharide, they activate M1 macrophages, which can secrete inflammatory factors, such as IL-6 and tumor necrosis factor-alpha, and can phagocytize invasive pathogens and tumor cells[23,26]. Hypoxia can also lead to immune escape through the role of immune cells[5]; for example, hypoxia can reduce T-cell activity[27]. Hypoxia is closely related to immune cell function. In our study, we observed significant differences in the levels of activated CD4 memory T cells and M0 macrophages between the high- and low-risk groups in TCGA database. In the GEO database, the levels of infiltration of activated CD4 memory T cells and M0 macrophages, those of activated and resting mast cells, and those of neutrophils differed significantly between the high- and low-risk groups. Both databases showed significant differences in the infiltration rates of activated CD4 memory T cells and M0 macrophages between the high- and low-risk groups. When we screened the genes that regulated these two kinds of cell function, we found different levels of *CCL2/4/5, CSF1*, and *CX3CL1* expression between the high- and low-risk groups. Further analyses confirmed the significant correlation between the expression level of each of these genes and the risk of hypoxia.

Three of these five genes encode chemokines, which play a chemotactic role in immune cells, such as natural killer cells and monocytes, which are closely related to tumor development. *CCL2* and *CCL5* play important roles in prostate cancer metastasis and drug resistance[28,29], while *CCL4* is associated with the clinical characteristics of breast cancer[30]. Previous studies have shown that *CX3CL1* can recruit natural killer T and dendritic cells to participate in antitumor immunity[31,32]. *CX3CL1* is expressed in various tumors[33–35]; however, its antitumor effects remain controversial. Specifically, Tsang[33] reported that *CX3CL1* expression was positively correlated with the rate of lymphocyte infiltration and negatively correlated with tumor survival. Colony-stimulating factor 1 is expressed in various tumor cells[36]. Its secretion can induce the differentiation of M2-type macrophages and recruit immune cells into the tumor[37]. The five genes identified in the present study are closely related to immune cells.

Conclusion

In conclusion, hypoxia plays an important role in the tumor microenvironment. Screening for genes that can affect the rate of immune cell infiltration revealed a correlation between these genes and the hypoxia risk score. Our findings show that hypoxia-related genes can affect the prognosis of intestinal cancer and may play a role in immune infiltration in intestinal cancer. Analysis of the relationship between hypoxia and immune cells may improve immunotherapy and tumor treatment.

Declarations

Ethics approval and consent to participate

The research didn't involve animal experiments and human specimens,no ethics related issues. All participants provided a signed informed consent.

Consent for publication

All the authors have read and approved the manuscript in all respects for publication.

Data availability

The data that support the findings of this study obtained from TCGA (https://portal.gdc.cancer.gov/) and GEO (gse39582) databases.

Competing interests

The authors declare that they have no competing interests.

Funding

Finance Department of Jilin(2018SCZWSZX-039);Finance Department of Jilin(JLSWSRCZX2020-083); Science and Technology of Jilin(20170623092TC-119).

Authors' contributions

The data analysis and original writing of the draft were conducted by Luping Zhang and Shaokun Wang. Hong Xu and Nan Zhang came up with the design and critical revision of the manuscript. The original writing of the draft and its editing were by Yachen Wang,Weidan Zhao and Yingli Zhang. All authors read and approved the final manuscript.

Acknowledgements

We would like to acknowledge the reviewers for their helpful comments on this study.

References

1. Stephen P. The distribution of secondary growths in cancer of the breast. Lancet. 1889;133(3421):571–3.
2. Hanahan D, Coussens Lisa M. Accessories to the Crime: Functions of Cells Recruited to the Tumor Microenvironment. Cancer Cell. 2012;21(3):309–22.
3. Lebleu VS. Imaging the tumor microenvironment. Cancer J. 2015;21:174–8.
4. Klemm F, Joyce JA. Microenvironmental regulation of therapeutic response in cancer. Trends in Cell Biology. 2015;25(4):198–213.
5. Barsoum IB, Koti M, Siemens DR, Graham CH. Mechanisms of hypoxia-mediated immune escape in cancer. Cancer Research. 2014;74(24):7185–7190.
6. Multhoff G, Vaupel P. Hypoxia Compromises Anti-Cancer Immune Responses. Advances in experimental medicine and biology. 2020;1232:131–143.
7. Chaturvedi P, Gilkes DM, Wong CCL, et al. Hypoxia-inducible factor–dependent breast cancer–mesenchymal stem cell bidirectional signaling promotes metastasis. The Journal of Clinical Investigation. 2013;123(1):189–205.
8. Cheng JC, Klausen C, Leung PCK. Hypoxia-inducible factor 1 alpha mediates epidermal growth factor-induced down-regulation of E-cadherin expression and cell invasion in human ovarian cancer cells. Cancer Letters. 2013;329(2):197–206.
9. Rankin EB, 2, Giaccia AJ. Hypoxic control of metastasis. Science. 2016(6282):175–180.
10. Facciabene A, Peng X, Hagemann IS, et al. Tumour hypoxia promotes tolerance and angiogenesis via CCL28 and T(reg) cells. Nature. 2011;475(7355):226–230.
11. Gavalas NG, Tsiatas M, Tsitsilonis O, et al. VEGF directly suppresses activation of T cells from ascites secondary to ovarian cancer via VEGF receptor type 2. British Journal of Cancer. 2012;107(11):1869–1875.
12. Franovic A, Gunaratnam L, Smith K, Robert I, Patten D, Lee S. Translational up-regulation of the EGFR by tumor hypoxia provides a nonmutational explanation for its overexpression in human cancer. Proceedings of the National Academy of Sciences. 2007;104(32):13092–13097.
13. Misra A, Pandey C, Sze SK, Thanabalu T. Hypoxia activated egfr signaling induces epithelial to mesenchymal transition (EMT). Plos One. 2012;7(11):e49766.
14. Wang Y, Roche O, Xu C, et al. Hypoxia promotes ligand-independent EGF receptor signaling via hypoxia-inducible factor–mediated upregulation of caveolin-1. Proceedings of the National Academy of Sciences. 2012;109(13):4892–4897.
15. Lin WR, Chiang JM, Lim SN, Su MY, Yeh CT. Dynamic bioenergetic alterations in colorectal adenomatous polyps and adenocarcinomas. EBioMedicine. 2019;44:334–345.
16. Bu P, Chen KY, Xiang K, et al. Aldolase B-Mediated Fructose Metabolism Drives Metabolic Reprogramming of Colon Cancer Liver Metastasis. Cell Metabolism. 2018;27:1249.
17. Melo SA, Luecke LB, Kahlert C, et al. Glypican-1 identifies cancer exosomes and detects early pancreatic cancer. Nature. 2015;523(7559):177–182.

18. Chamorro-Jorganes A, Araldi E, Rotllan N, Cirera-Salinas D, Suarez Y. Autoregulation of glypican-1 by intronic microRNA-149 fine tunes the angiogenic response to FGF2 in human endothelial cells. Journal of Cell ence. 2014;127(6):1169.
19. Pamidimukkala NV, Leonard MK, Snyder D, McCorkle JR, Kaetzel DM. Metastasis Suppressor NME1 Directly Activates Transcription of the ALDOC Gene in Melanoma Cells. Anticancer research. 2018(11):6059–6068.
20. Debangshu S, Semenza GL. Metabolic adaptation of cancer and immune cells mediated by hypoxia-inducible factors. Biochimica et Biophysica Acta (BBA) - Reviews on Cancer. 2018;1870:15–22.
21. JM B, AN M. M I, et al. Development and validation of a combined hypoxia and immune prognostic classifier for head and neck cancer. Clinical Cancer Research. 2019(17):5315–5328.
22. Yang L, Roberts D, Takhar M, et al. Development and Validation of a 28-gene Hypoxia-related Prognostic Signature for Localized Prostate Cancer. EBioMedicine. 2018:182–189.
23. Zhou D, Huang C, Lin Z. Macrophage polarization and function with emphasis on the evolving roles of coordinated regulation of cellular signaling pathways. CELLULAR SIGNALLING. 2014(2):192–197.
24. Sethi N, Kikuchi O, Mcfarland J, Zhang Y, Bass AJ. Mutant p53 induces a hypoxia transcriptional program in gastric and esophageal adenocarcinoma. JCI Insight. 2019;4(15):e128439.
25. Ning-Bo H, Mu-Han, et al. Macrophages in tumor microenvironments and the progression of tumors. Clinical & developmental immunology. 2012;2012:948098.
26. Murray PJ. Macrophage Polarization. Annual Review of Physiology. 2016;79(1):541.
27. Sun J, Zhang Y, Yang M, et al. Hypoxia induces T-cell apoptosis by inhibiting chemokine C receptor 7 expression: the role of adenosine receptor A2. Cellular & Molecular Immunology. 2010;7(1):77–82.
28. Urata S, Izumi K, Hiratsuka K, et al. C-C motif ligand 5 promotes migration of prostate cancer cells in the prostate cancer bone metastasis microenvironment. Cancer ence. 2018;109(3):724–731.
29. Targeting the androgen receptor with siRNA promotes prostate cancer metastasis through enhanced macrophage recruitment via CCL2/CCR2-induced STAT3 activation. Embo Molecular Medicine. 2013;5(9):1383–1401.
30. Hu G, Tzeng H, 3,4, Chen P, et al. Correlation between CCL4 gene polymorphisms and clinical aspects of breast cancer. International Journal Of Medical Sciences. 2018(11):1179–1186.
31. Guo J, Chen T, Wang B, et al. Chemoattraction, adhesion and activation of natural killer cells are involved in the antitumor immune response induced by fractalkine/CX3CL1. Immunology letters. 2003(1):1–7.
32. Guo J, Zhang M, Wang B, et al. Fractalkine transgene induces T-cell-dependent antitumor immunity through chemoattraction and activation of dendritic cells. International Journal of Cancer. 2003(2):212–220.
33. T JYS, Y.-B. N S-K, C, et al. CX3CL1 expression is associated with poor outcome in breast cancer patients. Breast Cancer Research and Treatment. 2013:1–10.

34. Celesti G, Di Caro G, Bianchi P. Early expression of the fractalkine receptor CX3CR1 in pancreatic carcinogenesis. BRITISH JOURNAL OF CANCER. 2013(9):2424–2433.
35. Xa Y, La Q, Xa C, Ja Du, Za Z, Sb L. Expression of CX3CR1 associates with cellular migration, metastasis, and prognosis in human clear cell renal cell carcinoma(Article). Urologic Oncology: Seminars and Original Investigations. 2014(2):162–170.
36. Shaposhnik SJP, JL S. Targeting distinct tumor-infiltrating myeloid cells by inhibiting CSF-1 receptor: combating tumor evasion of antiangiogenic therapy. Blood. 2010(7):1461–1471.
37. Dai X-M, Ryan GR, Hapel AJ, et al. Targeted disruption of the mouse colony-stimulating factor 1 receptor gene results in osteopetrosis, mononuclear phagocyte deficiency, increased primitive progenitor cell frequencies, and reproductive defects. Blood. 2002;99:111–120.

Figures

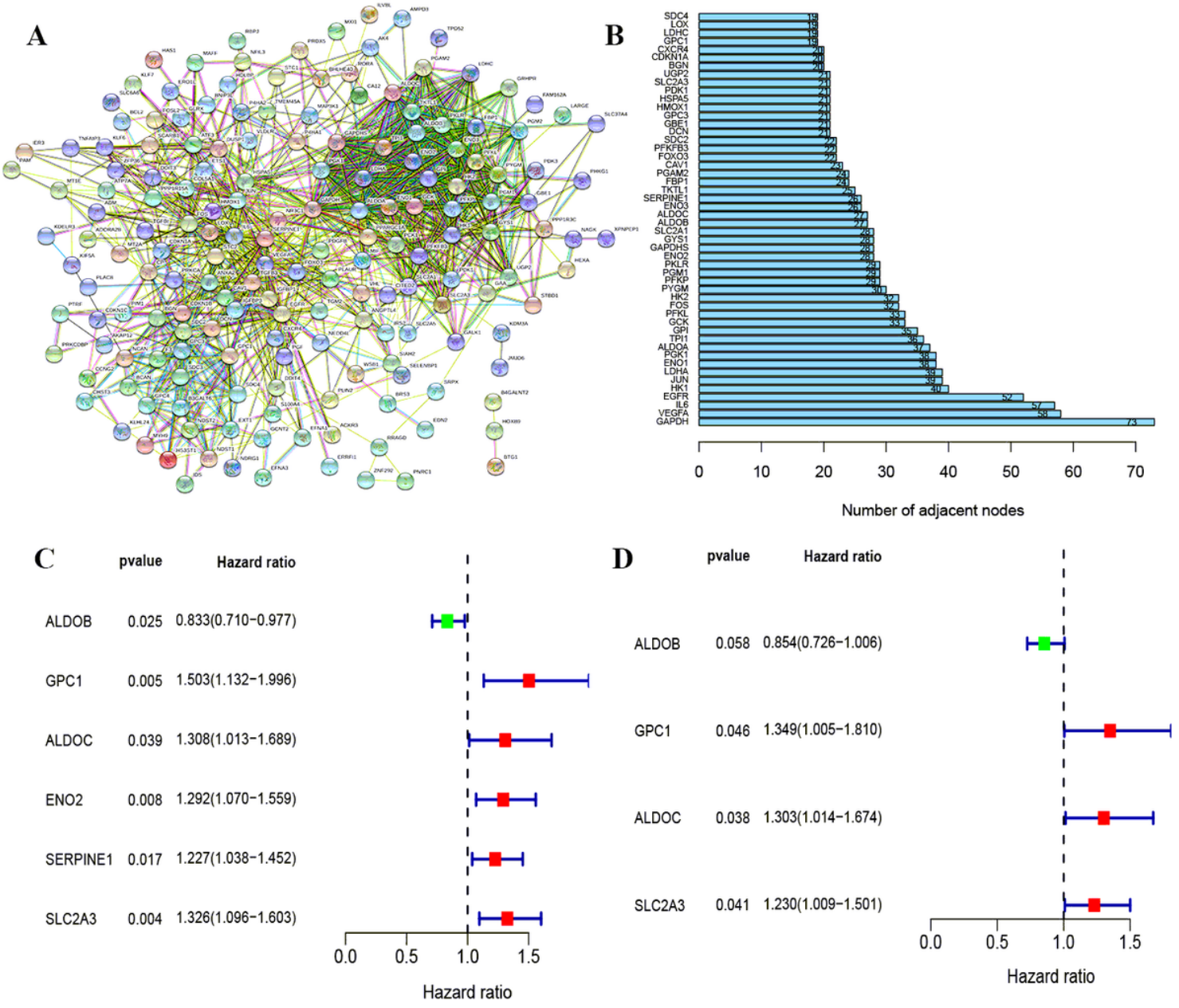

Figure 1

Screening for hypoxia-related genes and their relationship with patient prognosis. (A) Protein-protein interaction network containing members with interaction confidence values >0.4. (B) The top 50 genes selected based on the number of nodes and their sub-nodes. (C) Univariate Cox regression analysis identified candidate genes with p-values of <0.05. (D) Among the genes related to colorectal cancer prognosis, the genes shown are those independently related to patient prognosis in a multifactor prognostic model of hypoxia.

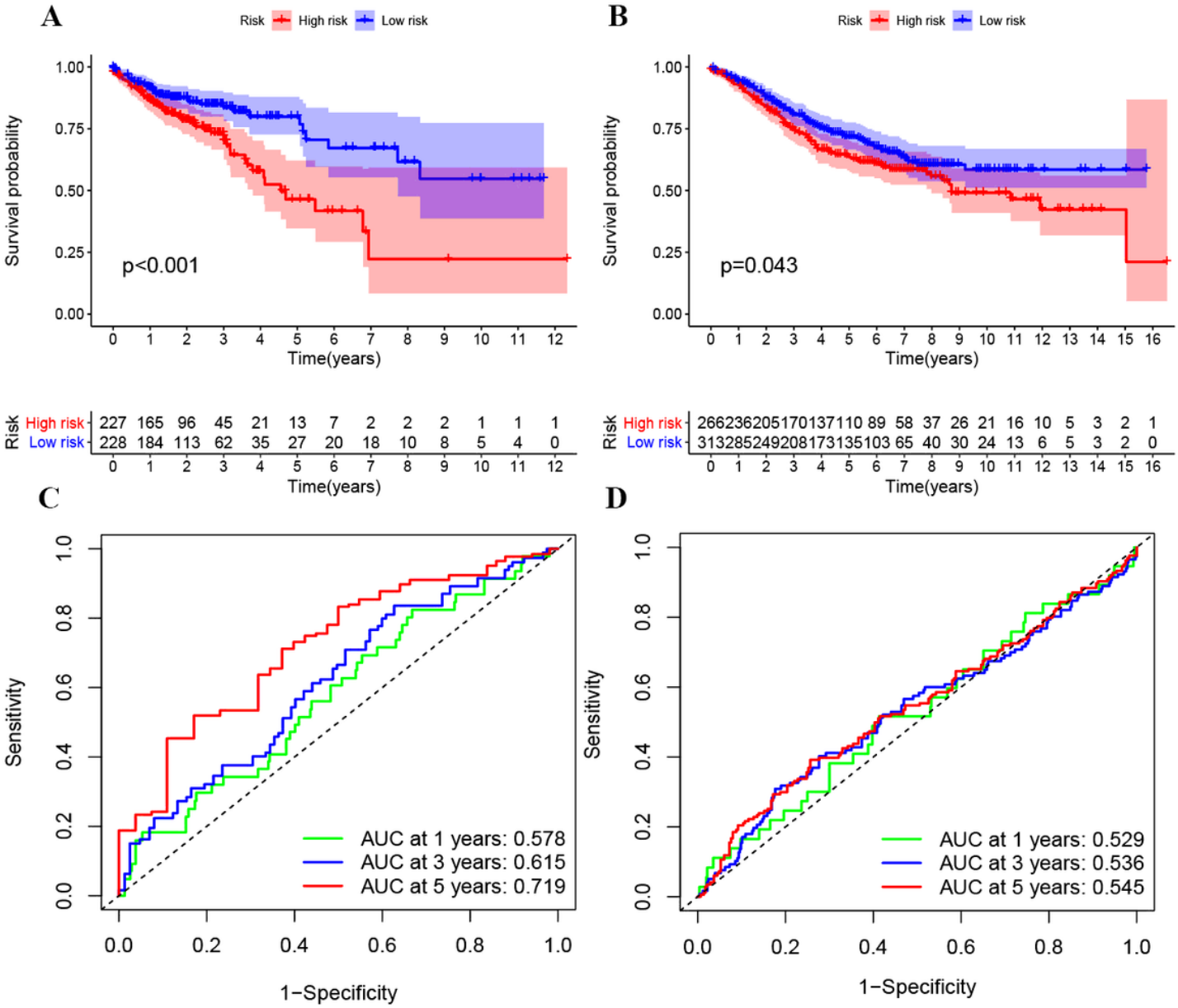

Figure 2

Effect of the hypoxia model on patient prognosis. (A–B) Kaplan–Meier survival curves for patients with colon cancer in The Cancer Genome Atlas (TCGA) and Gene Expression Omnibus (GEO) databases, stratified according to risk scores (high vs. low); comparisons of the median survival time in both groups

with log-rank tests (p□0.01 and p = 0.043, respectively). (C–D) Receiver operating characteristic curve analysis of the prognostic accuracy of the model. In TCGA database, the areas under the 1-, 3-, and 5-year survival curves gradually increased, while those in the GEO database did not change significantly over time.

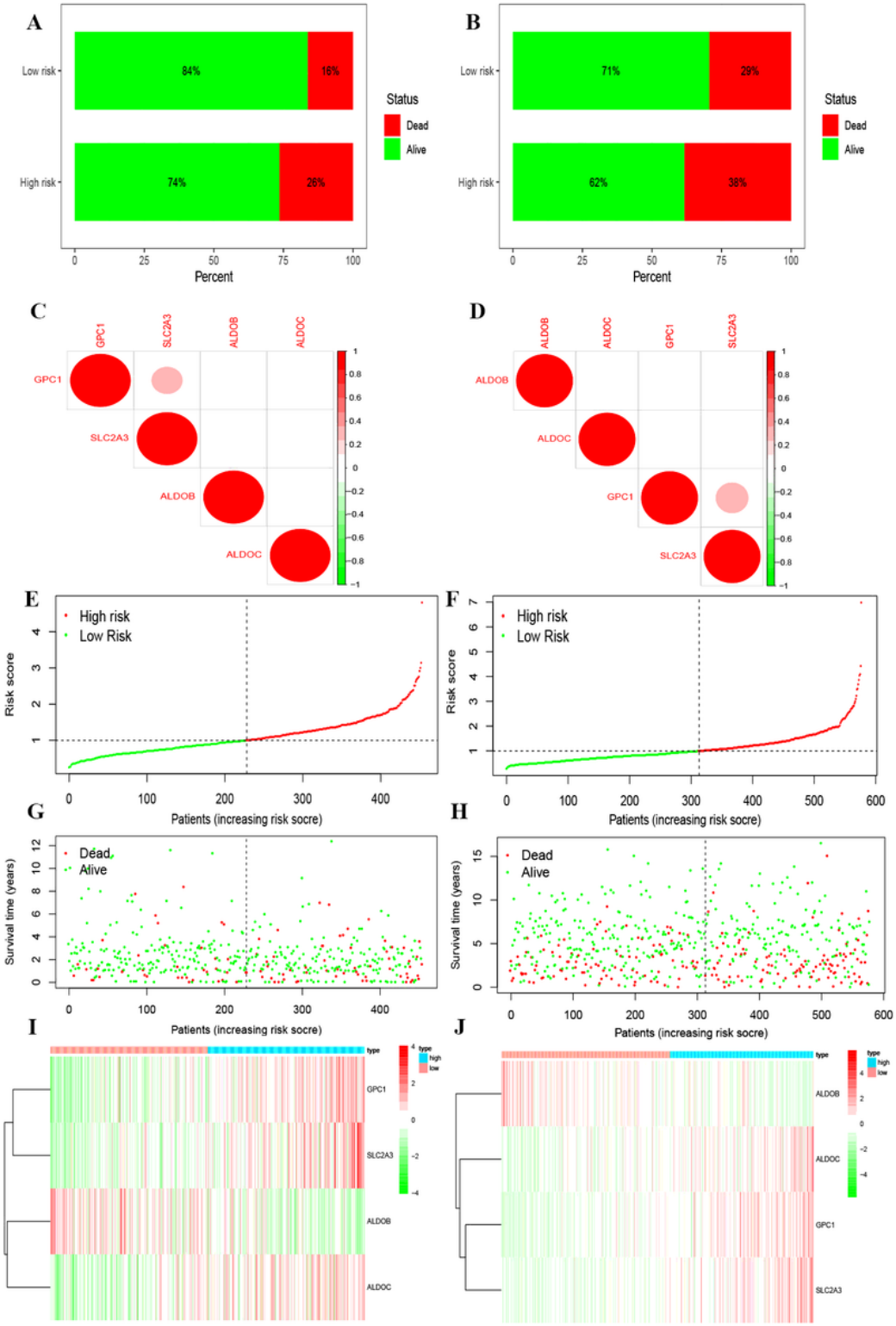

Figure 3

Prediction of patient risk in the hypoxia model and the expression levels of the genes included in the model. (A–B) Patient survival in The Cancer Genome Atlas (TCGA) and Gene Expression Omnibus (GEO) databases. (C–D) Correlations between the genes included in the risk model based on TCGA and GEO databases. Positive and negative correlations are indicated in red and green, respectively. (E–F) Patient risk scores in TCGA and GEO databases. (G–H) Survival rates in the high- and low-risk patient groups in TCGA and GEO databases. (I–J) Heat maps of gene expression levels in the risk models for the high- and low-risk groups in TCGA and GEO databases.

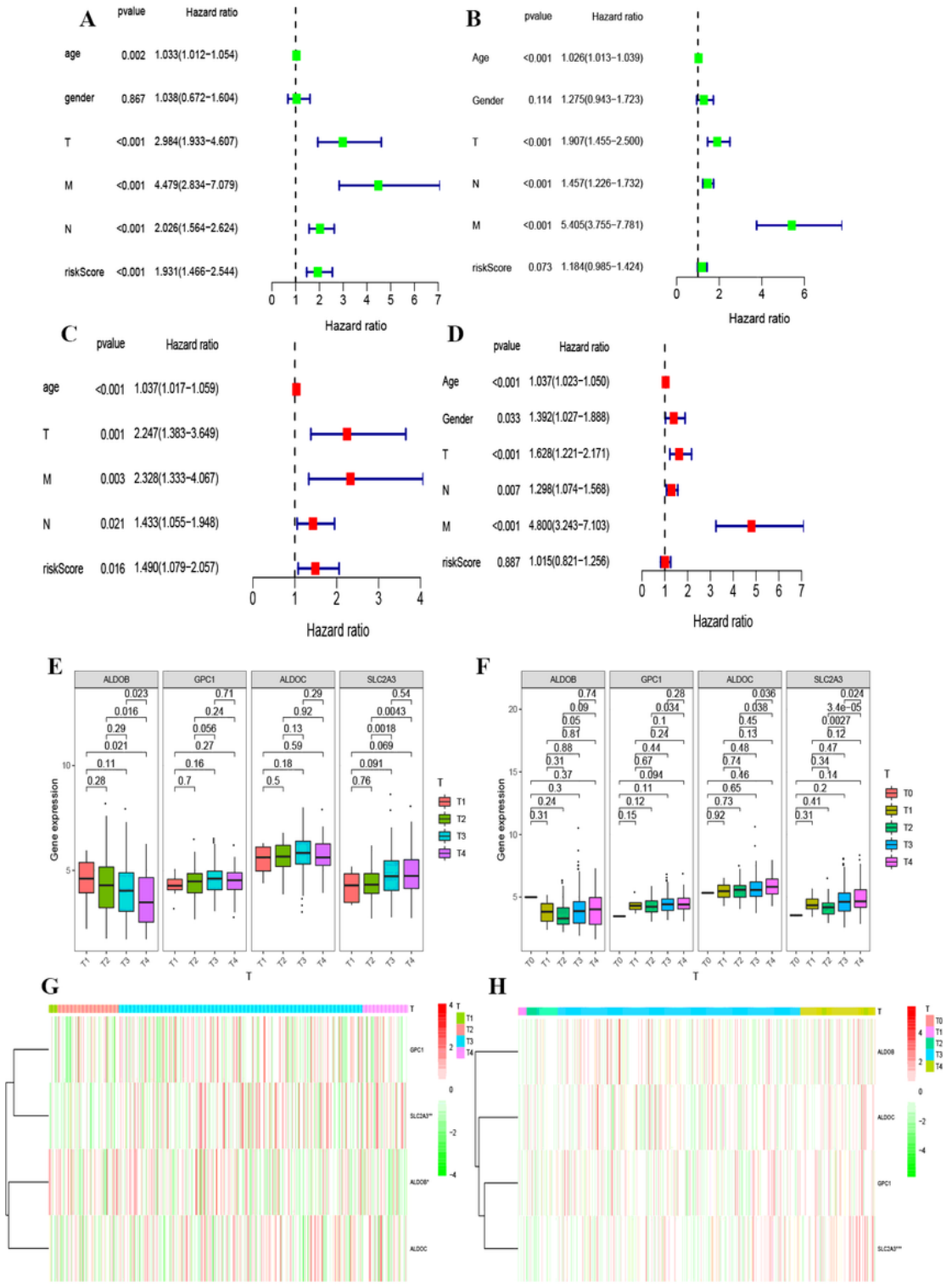

Figure 4

Relationships between risk models and clinical factors. (A–B) Single-factor prognostic analysis included age, sex, tumor–node–metastasis (TNM) stage, and the risk scores of patients with colorectal cancer in The Cancer Genome Atlas (TCGA) and Gene Expression Omnibus (GEO) databases. (C–D) Multi-factor prognostic analysis included age, sex, TNM stage, and the risk scores of patients with colorectal cancer in TCGA and GEO databases. (E–F) Comparisons of the expression levels of various genes in the hypoxia model in TCGA and GEO databases for different T stages. (G–H) Heat maps showing the expression levels of genes in the risk models in TCGA and GEO databases for different T stages.

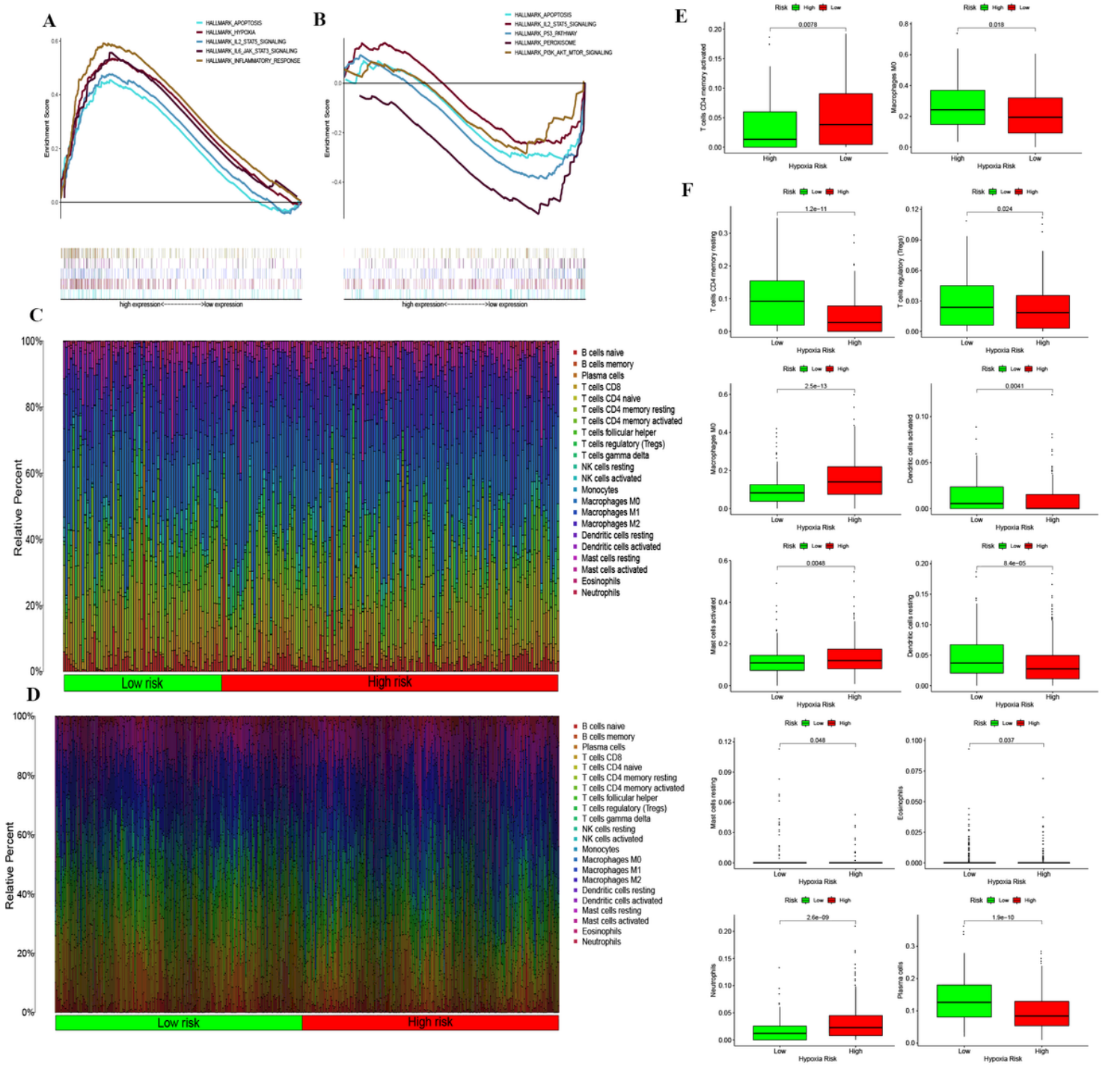

Figure 5

Enrichment of hypoxia pathways and infiltration of hypoxia-related immune cells. (A) Enriched gene sets in the HALLMARK collection according to high-risk scores in The Cancer Genome Atlas (TCGA) database. Each line represents one particular gene set with a unique color, with upregulated genes appearing on the left side approaching the origin of the coordinates and downregulated genes appearing on the right side of the x-axis. Only gene sets with nominal (NOM) p-values of <0.05 and false discovery rate (FDR) q values of <0.06 were considered statistically significant. A selection of leading gene sets is shown in the plot. (B) The enriched gene sets in the HALLMARK collection by low-risk scores in the Gene Expression Omnibus (GEO) database. Only gene sets with NOM p-values of <0.05 and FDR q values of <0.06 were considered statistically significant. A selection of leading gene sets is shown in the plot. (C) Heat map of hypoxia risk and immune cell infiltration in TCGA and GEO databases. (D) Immune cells whose infiltration is significantly associated with the risk of hypoxia in TCGA database ($p < 0.05$). (E) Immune cells whose infiltration is significantly associated with the risk of hypoxia in the GEO database ($p < 0.05$).

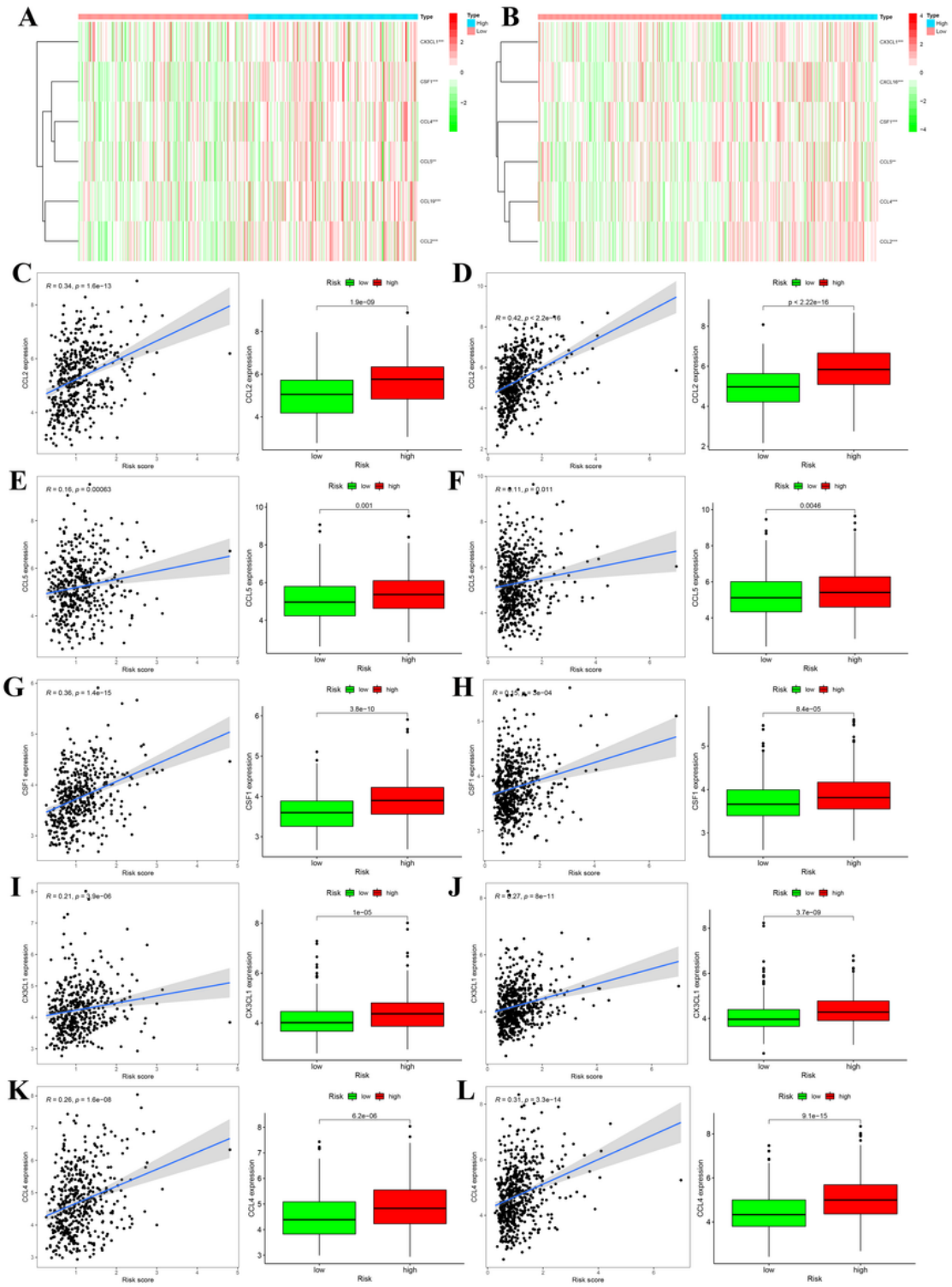

Figure 6

Relationships between genes regulating immune cell behavior and hypoxia risk. (A–B) Heat maps showing the expression levels of genes regulating activated CD4 memory T cells and M0 macrophages in different hypoxia risk groups (*p < 0.05; **p < 0.01; ***p < 0.001). (C–L) Scatter plots showing the correlations of the expression of five genes from The Cancer Genome Atlas and Gene Expression Omnibus databases with immune cell regulation, showing differences in the expression levels between

the different hypoxia risk groups ($p < 0.05$). The blue line in each plot is a fitted linear model indicating the relationship between gene expression and the risk of hypoxia. Pearson coefficients were used to assess the correlation between the two factors. The box plots show the differences in the levels of gene expression between groups at risk of hypoxia ($p < 0.05$).

Supplementary Files

This is a list of supplementary files associated with this preprint. Click to download.

- Stab.docx